Journal of Nuclear Materials 395 (2009) 89–98

Contents lists available at ScienceDirect

Journal of Nuclear Materials

journal homepage: www.elsevier.com/locate/jnucmat

Modelling of the spent fuel oxidation: Toward the operational model

J. Rouyer [a], A. Poulesquen [b,*], L. Desgranges [c], C. Ferry [a]

[a] Commissariat à l'Energie Atomique, DEN/DPC/SECR, Centre d'Etudes de Saclay, Bat 450 91191 Gif sur Yvette Cedex, France
[b] Commissariat à l'Energie Atomique, DEN/DTCD/SPDE, CEA d'Etudes de Marcoule, Bat 37, BP 17171-30207 Bagnols-sur-Cèze cedex, France
[c] Commissariat à l'Energie Atomique, DEN/DEC/SA3C, Centre d'Etudes de Cadarache, 13108 S[T] Paul les Durance, France

ARTICLE INFO

Article history:
Received 16 January 2009
Accepted 29 September 2009

ABSTRACT

As part of a long-lasting dry storage, the oxidation of the spent fuel linked to an accidental supply of oxygen into the spent fuel rod, may have consequences that must be assessed. Indeed, the oxidation of the UO_2 fuel up to U_3O_8 phase brings about a volume swelling of about 31% together with a bulking which may increase the initial defect of the cladding and thus lead to the release of fission products which remains embedded in nanometric gains or fine particles. From the oxidation model first developed (grain model), a new model has been proposed to describe the oxidation of spent fuel. The latter is based on a transposition of the graded grain model for unirradiated powders to irradiated grains. The modification of the grain model concerns the structural evolutions and the stoichiometric ranges during the oxidation. The convolution between the irradiated grain model and the propagation of the oxidation front along the grain boundaries allow to describe the oxidation kinetics of a spent fuel fragment. A criterion of grain breaking, based on experimental observations, has been proposed. The model has been parametrized from the experimental data of the literature and obtained as part of the French PRECCI's program. The harmony between the model and the experimental data either in terms of mass gain curves or of the oxygen diffusion coefficients in the UO_2 matrix is satisfactory. From this mechanistic model, an operational model for dry storage is proposed. On one hand, a simplified model (qualitative one) allowing to link the operational parameters (irradiation history) such as the burn up, the linear power or else the released gas fraction to a time for cracks to appear in the grains has been proposed. This model allows to display the time for the fractures in the fuel to appear (or a time before fracturing) according to the review of the treated fuels. On the other hand, a predictive operational model taking only the temperature into account is proposed.

1. Introduction

As far as a long-term dry storage is concerned, the oxidation of the spent fuel due to a supply of oxygen into the spent fuel rod have consequences that should be assessed. At dry storage temperatures (higher than 200 °C), UO_2 fuel in contact with air, oxidizes into U_3O_8, entailing a volumetric swelling of about 31% mainly corresponding to the decrease of the UO_2 density (10.99 g cm^{-3}) to that of U_3O_8 (8.34 g cm^{-3}). So, this solid-state swelling expected from the crystalline transformation and the bulking [1] (which can reach more than 300%) may increase the stress exerted on the rod and lead to the ruin of the fuel rod from one or several airtightness defects that may then spread. Moreover, a release of the radionuclides embedded in nanometric UO_2 grains (limited at 200 °C) or fine particles is expected due to the increase of the specific surface area. The oxidation mechanisms on unirradiated fuel and on spent fuel have been widely studied for the past 50 years. Detailed reviews on the oxidation tests realized on unirradiated or spent fuel are available in the literature [2,3]. Generally speaking the weight gain versus oxidation time curves can be divided into three phases: a near parabolic one sometimes with a sigmoidal shape disclosing an incubation time, a plateau and then another sigmoid part. The paper deals with the first two part up to the plateau.

Recently, significant progress in understanding the oxidation mechanism on virgin powder has been made. Indeed, during the first oxidation step (parabolic kinetics) two intermediate oxidation products U_4O_9 and U_3O_7 have been identified [4]. These observations have shown that the phases (UO_2, U_4O_9 and U_3O_7) coexisted in the first stages of oxidation with a series of structural phase changes as follows [4]:

$$UO_2 \rightarrow U_4O_9 \rightarrow U_3O_7 \rightarrow U_3O_8$$

* Corresponding author. Address: Commissariat à l'Energie Atomique, Centre d'Etudes de Marcoule, Département de Traitement et de Conditionnement des Déchets (DTCD), Service des Procédés de Décontamination et des Enrobages (SPDE), 30207 Bagnols-sur-Cèze cedex, France. Tel.: +33 (0)4 66 79 18 01; fax: +33 (0)4 66 39 78 71.
E-mail address: arnaud.poulesquen@cea.fr (A. Poulesquen).

0022-3115/$ - see front matter © 2009 Elsevier B.V. All rights reserved.
doi:10.1016/j.jnucmat.2009.09.023

These successive structural phases go with an evolution of the O/U ratio according to time and temperature. Generally, for temperatures below 300 °C, an oxidation plateau is reached when O/U ratio is equal to 2.33, which corresponds to U_3O_7 stoichiometric phase [5].

The structural evolution and the stoichiometric ranges of the phases appearing during the oxidation of the spent fuel are more difficult to determine because of the difficulties of handling the samples. Implementing is complicated if the evolution of the phases during oxidation is to be followed, which requires XRD measurements. The structural evolution commonly admitted in the literature concerning the spent fuel is the following:

$$UO_2 \rightarrow U_4O_{9+y} \rightarrow U_3O_8$$

So the intermediate phase U_4O_{9+y} is stabilized. This phase has a hyper-stoichiometric quadratic phase with an O/U ratio usually close to 2.4 rather than the nominal value of 2.25. The U_3O_7 phase is not observed in spent fuel because the precipitated fission products disturb the long-range order at a great distance of the oxygen atoms [6]. The hyper-stoichiometry of U_3O_7 is determined by the experimental weight gain curves. The experiments [7], carried out on spent fuel have also shown that spent fuel includes a U_4O_{9+y} phase. Usually, on UOX fuels, a value of 2.4 is obtained for the final O/U ratio of U_4O_{9+y}.

During its stay in a PWR, the spent fuel rod is subjected to interdependent neutronic, thermal, mechanical and physico-chemical phenomena that change the UOX and MOX pellets during their irradiation. Their chemical composition is modified by the formation of fission products and other actinides. The main operational parameter governing the radionuclide inventories is the burn up. Pellets also split into several fragments (15 on average). The microstructure of the pellet under irradiation is modified with the appearance of fission gas bubbles [8] followed by fission gas release toward the free volumes of the rods following the tunnels of diffusion [9]. The oxidation behaviour is thus specific to each type of fuel analysed according to its irradiation history which is characterised by the linear power, the burn up and the released gas fraction, and to its manufacturing process in particular the initial porosity.

It is difficult to draw a trend in the propagation of the oxidation front in fuel from literature reports nor it is possible to get clear conclusion about the stabilized phase at the oxidation plateau. Indeed, Wasywich et al. [10] carried out long-lasting oxidation experiments in air at 150 °C on Canadian spent fuels (CANDU). The samples burn up lied between 7 and 8.5 GWd t^{-1} and the linear power ranged between 330 and 500 W cm^{-1}. The oxidation began at free surfaces (fractures) and progressed along the grain boundaries. Then, from the grain boundaries, a layer of higher oxide U_3O_7 grew inward from the external surface of the grain. The oxidation front spread homogeneously in the fragments, (Fig 1a). For American or French PWR fuels the stabilized oxidized phase observed is usually U_4O_9 hyper-stoichiometric [2]. This structural difference is explained by a burn up effect. Indeed, the burn up values reached by American and French fuels are 4 to 10 times higher than those of CANDU fuels, which means a significant increase of fission products which could stabilize the quadratic phase U_4O_{9+y}.

At temperature between 170 and 250 °C, another oxidation behaviour is observed in American PWR fuels presenting a burn up between 20 and 40 GWj t^{-1} and linear powers of about 170–200 W cm^{-1} [2,11,12]. It is hypothesized that the grain boundaries oxidize much faster than the grains. The transport of oxygen is made easier by the presence of fission gas bubbles generated in reactor at the grain boundaries (Fig. 1b). Nevertheless, Thomas et al. [13] notice that although most of their samples show a regular oxidation of the grain boundaries, locally some areas do not seem to be "attacked" by oxygen.

French PWR fuels, which generally have a burn up between 45 and 70 GWj t^{-1} for linear powers of about 150 W cm^{-1}, have revealed [7]:

- The existence of tunnels enabling the fast spreading of oxygen in the spent fuel fragments. This explains the local spreading of the oxidation front in Fig. 1c.
- The probable existence of a gas release simultaneous to weight gain.

The propagation of oxygen into the irradiated ceramic can thus occur in the gaseous phase along the fractures and cracks, or through the so-called "open" grain boundaries, fragilized by irradiation, or else by the tunnels generated during irradiation by the fission gases. Of course the oxygen also spreads by solid-state diffusion along the so-called "closed" grain boundaries and in the bulk of the grains.

The ratio of both rate (gas/solid phase) impacts the weight gain curves. It is illustrated by Fig. 2a and b. When the oxidation rate at grain boundaries is largely superior to that in the grain, a parabolic shape of the weight gain curve is observed (Fig. 2b) except perhaps for the Turkey Point data which present a slight inflexion at the beginning of the experiment. The fragment thus considered behaves as a powder: the weight gain curve in Fig. 2a corresponds to Fig. 1b. Yet when the oxidation rate at grain boundaries is just enhanced locally [7], or equal [10] to bulk diffusion, a moderate inflection is observed at the beginning of oxidation: the Fig. 2b is represented by Fig. 1c.

In order to describe these various oxidation behaviours, some laws are available in the literature. In general, stationary laws such

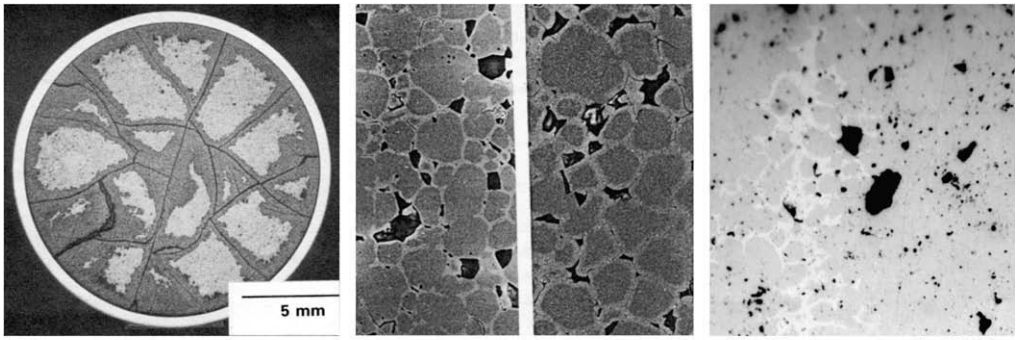

(a) – Wasywich et al. (1992) [9] (b) – Einziger et al. (1992) [10] (c) – Desgranges et al. (2007) [6]

Fig. 1. Different ways of oxygen propagation in the spent fuel according to the irradiation history (photos from [6,9,10]).

as Jander's are used to interpret the transition of UO_2 toward U_4O_9/U_3O_7. Non-stationary laws are also used but only to describe the transition $UO_2 \rightarrow U_3O_7$. These laws do not take into account the structural evolution observed in unirradiated UO_2 powders as do not describe the incubation time neither nor the evolution at the oxidation plateau observed on the weight gain curves of the spent fuel. Moreover, no link between the law parameters and the irradiation parameters (burn up, linear power and release gas fraction) of irradiated samples are made.

In order to take into account the structural evolution observed on unirradiated powder, a grain model has been developed [14]. Then, a description of the oxidation kinetics observed on irradiated fuels has been proposed. The model rests on taking into account the two phenomena discussed beforehand namely the oxidation at the grain boundaries and the grain bulk oxidation [15]. One must notice that the model only describes the oxidation kinetics up to the oxidation plateau.

The goal of this paper is firstly to describe the kinetics of the spent fuel weight gain curves at various temperatures using the grain model already available and the convolution process between this grain model and the oxidation front propagation rate along the grain boundaries. Secondly, the determination of a time for the first cracks to appear in the grains, based on new experimental results [16], is proposed.

The parameters of this model, based on the diffusion mechanisms of oxygen in the nuclear ceramic, are fitted on the experimental data available in the literature. An operational model is proposed. It is a simplified model enabling to link the time for cracks to appear in the grains to operational parameters such as burn up, linear power and release gas fraction.

2. Description of the model

2.1. The grain model

To take into account the new experimental observations concerning the structural evolution during the oxidation kinetics ($UO_2 \rightarrow U_4O_9 \rightarrow U_3O_7$), a numerical model based on the finite differences method has been proposed [14].

The method adopted is the modelling of two non-stationary superposed and interdependent oxidation fronts U_4O_9 and U_3O_7. Discretisation is performed on a sphere of radius R with spatial and time steps dr and dt, respectively. The convergence condition of the numerical method is expressed by:

$$2D \leqslant \frac{dr^2}{dt} \tag{1}$$

(this must be verified for the two rates of oxygen diffusion in U_4O_9 and U_3O_7 phases, $D_{U_4O_9}$ and $D_{U_3O_7}$, respectively)

The model is based on the step by step resolution of the Fick's law in spheric coordinates:

$$\frac{\partial C}{\partial t} = D\left(\frac{2}{R}\frac{\partial C}{\partial r} + \frac{\partial^2 C}{\partial r^2}\right) \tag{2}$$

When the concentration at reaction interfaces reaches a sufficient value, the new phase is formed (sub-stoichiometric U_3O_7 or U_4O_9). The driving force of diffusion is the stoichiometric gradient in the two phases. The calculation starts with an initial layer of U_4O_9 at the surface (Fig. 3). The model parameters are the stoichiometries at the interfaces of the two phases U_4O_9 and U_3O_7 and the diffusion coefficients of oxygen $D_{U_4O_9}$ and $D_{U_3O_7}$. Diffusion coefficients are obtained by fitting the weight gain on experimental data from CEA and literature [14].

The stoichiometric ranges are established from thermodynamic data:

- U_4O_9: [2.22–2.25]
- U_3O_7: [2.32–2.33]

2.2. The spent fuel oxidation model

2.2.1. Phenomenology

As mentioned in the introduction, the spent fuel oxidation is the result of two phenomena schematized on Fig. 4.

2.2.1.1. Oxidation of grain boundaries. The model convolutes the progression of the oxidation front in the grain with its progression along the grain boundaries. The oxidation rate along the grain boundaries is supposed to be constant. It does not depend on the radius of the fragment. It is expressed by:

$$\begin{aligned} R_{\text{advancement}} &= R_{\text{fragment}} - \frac{t.R_{\text{fragment}}}{t_0} \quad \text{for } t = [0; t_0] \\ &= 0 \quad \text{elsewhere} \\ v &= \frac{R_{\text{fragment}}}{t_0} \end{aligned} \tag{3}$$

with,

- t_0: the time for the oxidation front to reach the sphere centre (=fragment);
- $R_{\text{advancement}}$: the radial position of the oxygen front in the grain;
- R_{fragment}: the radius of the fragment;
- v: the rate at grain boundaries.

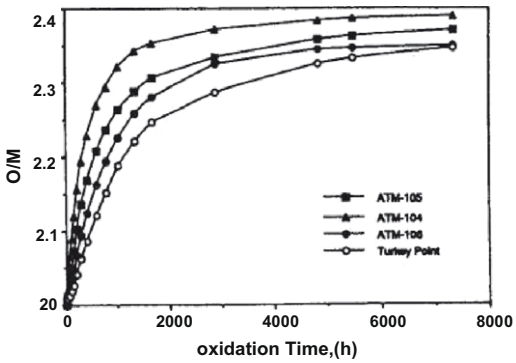

(a) : PWR US spent fuel. $V_{gb} >> V_g$. Einziger et al. (1992). [10]

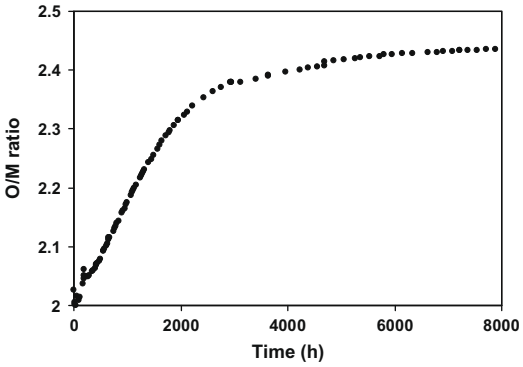

(b) : PWR French spent fuel. $V_{gb} >> V_g$ locally. Desgranges et al. (2007) [6]

Fig. 2. Shape of the weight gain curves according to the irradiation history (V_{gb} = oxidation rate at grain boundaries; V_g = oxidation rate in the grains).

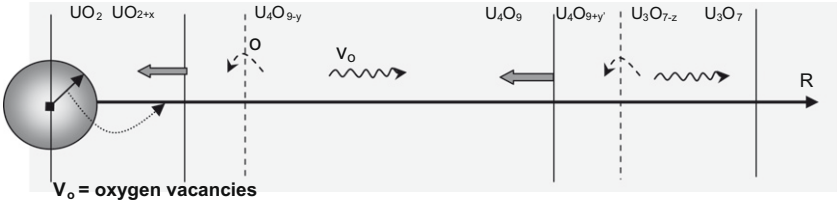

Fig. 3. Schematization of a grain oxidation model [13].

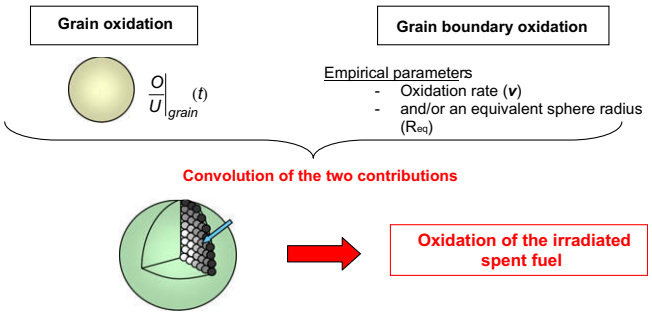

Fig. 4. Description of the convolution between the grain and grain boundary models.

2.2.1.2. Equivalent sphere. The fragment of spent fuel is more or less important microcracked depending on the linear power of the rod. Microcracks are akin to fission gas diffusion tunnels generated under irradiation. As a consequence, they enhance oxygen diffusion. To integrate this phenomenon into the modelling, the fragment radius is replaced by an equivalent radius (R_{eq}) in Eq. (4). The smaller the ratio $R_{eq}/R_{fragment}$ is, the higher the linear power undergone by the fuel in reactor is. This notion of equivalent sphere is also used for the models of gas release in reactor [17,18]. The modified oxidation model becomes:

$$\begin{aligned} R_{\text{advancement}} &= R_{\text{eq}} - \frac{t.R_{\text{eq}}}{t_0} \quad \text{for } t = [0; t_0] \\ &= 0 \quad \text{elsewhere} \\ R_{\text{eq}} &= V_{\text{gb}} t_0 \end{aligned} \tag{4}$$

with, R_{eq} is the radius of equivalent sphere and V_{gb} is the oxidation propagation at the grain boundaries. It is considered as a constant in the model because of the lack of experimental data on this subject. The equivalent sphere radius is then calculated from time estimation (t_0) to reach the centre of the sphere.

Finally, to describe the spent fuel weight gain curve, a numerical convolution between the grain model and the progression front of oxidation described by Eq. (4) is carried out.

2.2.2. Transposition unirradiated/irradiated for the grain oxidation model

During spent fuel oxidation tests, U_3O_7 phase is not stabilized because of a large number of fission products in the ceramic matrix. U_4O_9 hyper-stoichiometric phase is detected by XRD. Nevertheless, an analogy with the structure of the unirradiated fuel phases has been adopted for the spent fuel. It is justified from a structural point of view: in non-irradiated fuel, the change from UO_2 to U_4O_9 and from U_4O_9 to U_3O_7 observed during the oxidation is due to the accumulation and accommodation of additional oxygen atoms in cuboctahedral clusters which are centred on holes in the fluorite lattice [19–20]. In irradiated fuels, the accumulation of cuboctahedral during oxidation occurs but because of the presence of defects (FP), only U_4O_9 hyper-stoichiometric phase is observed.

The model is thus modified in the following way for irradiated fuels: the first phase apparition in the unirradiated fuel (U_4O_9) is kept whereas the U_3O_7 phase formation is transposed into U_4O_{9+y} apparition. The succession of phase change in irradiated fuel is:

$$UO_2 \rightarrow U_4O_9 \rightarrow U_4O_{9+y} \rightarrow U_3O_8$$

The oxidation mechanisms are similar between the unirradiated fuel and the spent fuel since it is the same matrix. As a consequence, the oxidation model of unirradiated grain can be adapted to an irradiated grain by modifying stoichiometric ranges according to the following figures:

- U_4O_9: [2.2–2.25],
- U_4O_{9+y}: [2.32 to ~2.4] (the choice of the upper limit is detailed later on).

2.3. Model parameters

2.3.1. The oxidation plateau value

The O/M ratio for the oxidation plateau seen on weight gain curve normalized to the initial sample weight is not easy to predict. Indeed, during experiments the maximal weight gains differs from one sample to another according to the irradiation history [7]. The oxidation plateau could be sensitive to the release of intergranular gas in reactor which increases with linear power. Indeed, a sample which has released all its intergranular gas while inside the reactor reach a higher value of oxidation plateau than a sample that retains some intergranular gas. As a consequence, the higher the linear power, the more important the fraction of gas released and so the higher the oxidation plateau. It also seems that the size of the sample has an influence on the maximal weight gain [7]. Moreover, it has been shown recently that the release of intergranular fission gas is proportional to the progression of the oxidation front along the grain boundaries for UOX fuels [21]. An important Fission Gas Release (FGR) implies a higher weight gain and thus can entail a higher value of the oxidation plateau reached during oxidation.

The weight gain is translated into the ratio (oxygen upon uranium) using the following equation:

$$\frac{O}{M} = 2 + \frac{M_{\text{U}}}{M_{\text{O}}} \frac{\Delta m}{m_{\text{initial}}} \tag{5}$$

with,

- M_U and M_O, the molar masses of uranium 238 and of oxygen 16;
- Δm, the mass variations during oxidation;
- O/M the ratio of the oxygen mole number to the number of moles of uranium.
- $m_{initial}$, the sample initial mass.

Using the sample global mass also means considering the fission products mass which should not be included in the calculation of the UOX stoichiometric phases. This slightly distorts the plateau value experimentally measured.

In the case of the spent fuel oxidation model, the stoichiometry of the phase U_4O_{9+y} range from 2.25 to 2 + P.

2.3.2. Summary of the model input and output parameters

The parameters of the model are gathered and annotated in Table 1. Their numerical values are obtained by fitting experimental weight gain curves from selected experimental data sets.

3. Intercomparison model/experiments

3.1. Presentation of the selected experimental data

Many oxidations of unirradiated powder have been done to study the behaviour of spent fuels during transport and dry storage. Experimental conditions are very restrictive when dealing with spent fuels. For this reason, the literature includes few studies on spent fuel compared with unirradiated material. For this study a maximum of weight gain curves of the UOX spent fuel at 473 K are required. The literature most often provides experiments carried out at temperatures higher than or equal to 573 K because at that temperature oxygen diffusion is accelerated which limits the duration of the experiment.

Part of the selected results comes from the CEA centers of Grenoble and Cadarache [7]; the others come from publications [2,11,22]. Choosing the data also concerned the differences in the samples treated in term of burn up, linear power, release gas fraction and oxidation temperature. These data are shown in Table 2. In every case they concern UOX fuel.

Table 1
Input and output parameters of oxidation model for spent fuel fragments.

Input parameters	R = grain radius P = plateau value $D_{U_4O_9/U_4O_{9+y}}$ = oxygen coefficient in the U_4O_9 et U_4O_{9+y} phases ε fixed at 0.1 = percentage defining the stoichiometry of fracture appearance V_{jdg} = oxidation rate at grain boundaries t_0 = time to reach the centre of the fragment
Out parameters	R_{eq} = equivalent sphere radius t_{frac} = time of the first crack appearance in the grains

3.2. Comparison with the model

Fig. 5 concerns Cadarache samples RE2 and RE3. Although they come from the same material, the value of RE3 plateau is lower than that of RE2. It seems that a gas release occurred around 9000 h for RE3 resulting in a loss of mass occurring at t = 10,000 h. Comparison of experience with modelling is satisfactory: the sigmoidal shape expected meaning a good description of incubation time is found together with a non zero weight gain on the plateau (in particular RE2). The small increase of the weight gain in the plateau phase makes the comparison with the literature models impossible (Jander or non-stationary laws) as explained elsewhere [5].

The Grenoble samples LB515 to LB518 are similar in size and origin. As a consequence, Fig. 6 shows that their weight gain curves are extremely similar. The model adjusts well with the beginning of the oxidation into U_4O_9 phase, and the beginning of the plateau is well described. Yet the model does not reproduce the important weight regain occurring at about 4000 h. This sudden increase of atomic ratio O/M around 4000 h is difficult to explain physically and as a consequence can not be correctly modelled with the model hypotheses. It is also noticed that the plateau value is quite high.

As for the experiments performed at Cadarache, the temperature is 473 K. The weight gain of samples LB is very fast compared to samples RE. LB linear power is 28.7 kW m^{-1} whereas RE is 17.2 kW m^{-1} (Table 2). This difference of linear power undergone in reactor may explain the faster kinetics at the beginning of oxidation and the value of the plateau. Indeed, LB linear power being high compared to the other samples of the panel, might result in a tunnel network and a larger opening of the grain boundaries. This tunnel network favours the progression of oxygen in the fragment thus reducing the incubation time before weight gain resulting in a sigmoid shape not so clear in Fig. 6.

The description by the model of the experiments made by Einziger et al. [11] is proposed Fig. 7 for a temperature of 468 K

Table 2
Review of the experimental data selected.

Literature data	Type	Burn up (GWj t^{-1})	Linear power (kW m^{-1})	Released gas fraction	Theoretical density	T (K)
Einziger ATM-104 [10]	Powder and little fragments ~100 mg	~43.00	21.00	1.10%	94 à 96%	468
Einziger ATM-105 [10]	Powder and little fragments ~ 100 mg	~28.00	~17.00	0.60%	95%	468
Einziger ATM-106 [10]	Powder and little fragments ~ 100 mg	~48.00	NA	17.70%	92 à 94%	468
Einziger Turkey Point [10]	Powder and little fragments (big grains) ~ 100 mg	~27.00	~18.20	<0.3%	92%	468
Cadarache-RE2 [6]	Big fragments	64.00	17.20	2.82%	NA	473
Cadarache-RE3 [6]	Little fragments	64.00	17.20	2.82%	NA	473
Grenoble-LB515 [6]	Fragments ~ 3000 μm	41	28.70	NA	NA	473
Grenoble-LB516 [6]	fragments ~ 3000 μm	41	28.70	NA	NA	473
Grenoble-LB517 [6]	Fragments ~ 3000 μm	41	28.70	NA	NA	473
Grenoble-LB518 [6]	Fragments ~ 3000 μm	41	28.70	NA	NA	473
Woodley-RUN1 [18]	Fragments ~ 195.2 mg	23.40	NA	<0.3%	92%	498
Woodley-RUN2 [18]	Fragments ~ 228.5 mg	23.00	NA	<0.3%	92%	498
Woodley-RUN5 [18]	Fragments ~ 214.6 mg	23.80	NA	<0.3%	92%	498
Woodley-RUN6 [18]	Fragments ~ 211.5 mg -	23.80	NA	<0.3%	92%	498
Hanson ATM-105-05 [1]	Fragments	29.20	~17	0.60%	95%	528
Hanson ATM-105-01 [1]	Fragments 183.63 mg	28.00	~17	0.60%	95%	556
Hanson ATM-105-03 [1]	Fragments 207.11 mg	28.10	~17	0.60%	95%	581

NA = not available.

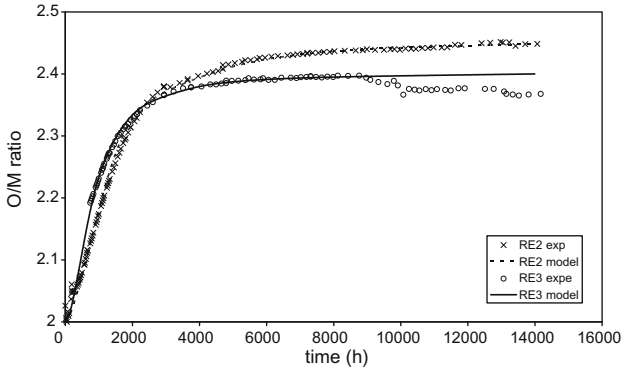

Fig. 5. Comparison between the calculation and the experimental CEA data (1), oxidation temperature = 473 K [6].

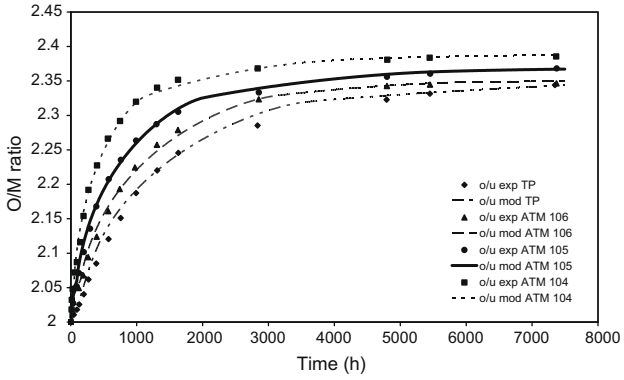

Fig. 7. Comparison between the calculation and the experimental Einziger et al. data [10], oxidation temperature = 468 K.

(Fig. 2a). The samples come from distinct rods with various burn up and linear power. These operational parameters and the size of the samples are likely to explain the various kinetics observed during oxidation. For example, a single curve presents a sigmoidal shape (TP = Turkey Point fuel) whereas the other three curves are parabolic. The spent fuel is always a mixture of powder and small fragments but the size of the TP's samples grains is bigger. The proportions of powder and fragments making each sample are detailed. Considering the experimental results, it might be expected that TP sample has a higher volume fraction of fragments.

ATM-104 is the sample which oxidises the fastest. It is consistent with the highest value of linear power as reported in Table 2. At the end of the experiment (~7500 h) the plateau value is quite weak. It could probably be ascribed to the gas release during oxidation which decreases the plateau value. ATM-106 oxidation can not be described using our model. Indeed, considering the FGR values given in Table 2 (the linear power is not given), the weight gain curve should show a fast oxidation at the beginning of the experiment and a plateau value higher than the other samples. Unfortunately, a lack of data inhibits any conclusion. Nevertheless, the plateau value can be correlated with FGR: ATM-104 (FGR = 1.1%) above ATM-105 (FGR = 0.6%), above Turkey Point (FGR < 0.3%). The modelling of this series of experiments is particularly good. Later on, the fact of considering a sample as a powder or as a fragment will be discussed.

Woodley et al. experiments [22] were carried out at 498 K. Data from these experiments are shown in Fig. 8. The shape of the curves is characteristic of the oxidation of irradiated fuel with a slight delay time for each sample. The samples come from the same fuel rod giving identical operational parameters (the linear power is not indicated, Table 2). The authors have chosen the size of the spent fuel fragment in the samples as variable parameters of their experiments. Specimen RUN 1, containing powder, has a small incubation time and the fastest oxidation rate at the beginning. On the opposite, specimen RUN 2 which is made up of an entire fragment shows a longer incubation period. This series of experiments presents the drawback of having been done on a short period. As the temperature accelerates weight gain kinetics, no point could be taken to give an information on the plateau. Nevertheless, the confrontation calculation/experiment is quite good whatever the samples.

The weight gain curves presented on Fig. 9 correspond to oxidation data from Hanson [1] at temperature of 528 K for sample ATM-105-05, 558 K for ATM-105-01, 581 K for ATM-105-03. At 558 and 581 K, we find again the classical shape of the oxidation kinetics curves observed at high temperatures with an intermediate plateau which nearly disappears (in particular for sample ATM-105-03). The grain model stops at the U_4O_{9+y} phase since the transition to U_3O_8 would require to couple oxidation with the mechanics of grain fragmentation. It is then impossible to model the weight gain after the first plateau. At these temperatures, the duration of the experiments was reduced by ten. The linear power and the burn up for each series are very similar since the samples come from the same fuel rod. The temperature is the operational parameter explaining the large variation between the kinetics. A good agreement between the calculation and the experiment is noted for the different temperatures.

In Table 3 the values of the model input parameters used to simulate each experiment are reported. The values of the diffusion coefficients of the two phases are obtained by adjustment of the grain model. About one order of magnitude separates $D_{U_4O_9}$ and

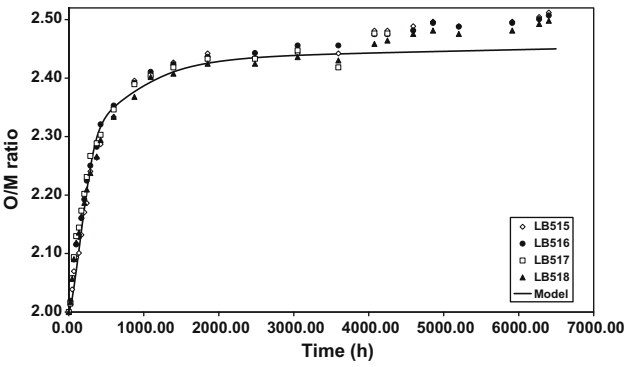

Fig. 6. Comparison between the calculation and the experimental CEA data (2), oxidation temperature = 473 K [6].

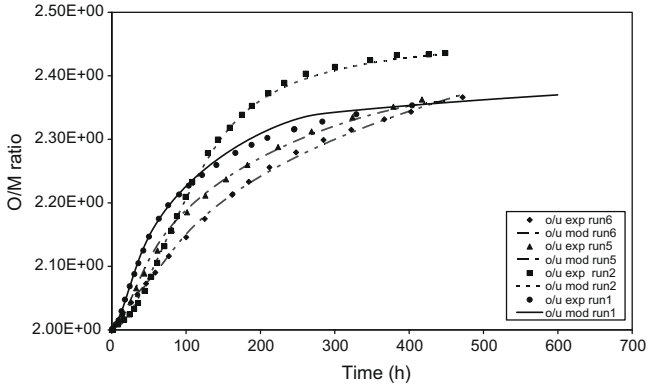

Fig. 8. Comparison between the calculation and the experimental Woodley et al. data [10], oxidation temperature = 498 K.

$D_{U_4O_{9+y}}$. The values of the oxidation plateau are also obtained from experimental curves.

3.3. Oxygen diffusion coefficients and activation energy

Diffusion coefficients of oxygen in U_4O_9 and U_4O_{9+y} are plotted versus inverse temperature in Fig. 10. Activation energies Ea and pre-exponential terms D_0 are calculated by a linear regression:

$$E_a^{U_4O_9} = 74.7 \text{ kJ mol}^{-1} \quad D_0^{U_4O_9} = 6.68 \times 10^{-10} \text{ m}^2 \text{ s}^{-1}$$
$$E_a^{U_4O_{9+y}} = 111 \text{ kJ mol}^{-1} \quad D_0^{U_4O_{9+y}} = 7.80 \times 10^{-7} \text{ m}^2 \text{ s}^{-1}$$

The values of activation energies agree with the literature data since their average worth 92.8 kJ.mol^{-1} and McEachern and Taylor [3] give a result of 95.7 kJ.mol^{-1} for a single oxidation stage. During the parameterization of the model on the unirradiated sample [14], the activation energies and the pre-exponential terms were calculated for U_4O_9 and U_3O_7 phases:

$$E_a^{U_4O_9} = 57 \text{ kJ mol}^{-1} \quad D_0^{U_4O_9} = 1.36 \times 10^{-9} \text{ m}^2 \text{ s}^{-1}$$
$$E_a^{U_4O_{9+y}} = 123 \text{ kJ mol}^{-1} \quad D_0^{U_3O_7} = 1.16 \times 10^{-3} \text{ m}^2 \text{ s}^{-1}$$

The larger value of $E_a^{U_4O_9}$ in the spent fuel compare to the unirradiated can be explained by the difficulty of diffusing oxygen in a matrix containing elements such as fission products and minor actinides [23]. As a consequence, it is necessary to provide more energy to the system to take that "tortuosity" into account.

It is interesting to note on the Fig. 10 that oxygen diffusion coefficients in both phases become similar at high temperature. That result is interesting since, for the unirradiated sample, when $T > 573$ K, there is no first oxidation plateau and the same phenomenon occurs on spent fuel. at a given temperature the results obtained for the diffusion coefficients are quite spread. This point is discussed in the Section 4.

3.3.1. Time to fracture the grains

Fracture is the first event of a series of mechanisms that finally leads to the transformation of the matrix into a very easily dispersed powder. To determine that moment, recent studies [16] on oxidation performed by XRD and ESEM on unirradiated mono and poly-crystals at temperatures between 250 and 370 °C showed that the first cracks appeared in the U_3O_7 phase (i.e. at the oxidation plateau) and not in the U_3O_8 phase as reported in the literature. The cracks appear for a critical thickness of U_3O_7 phase of less than a micron [16]. Complementary studies concerning the fracturation of UO_2 grains are being made. Yet, it is important to note that these results are obtained on unirradiated powders and not on irradiated grains.

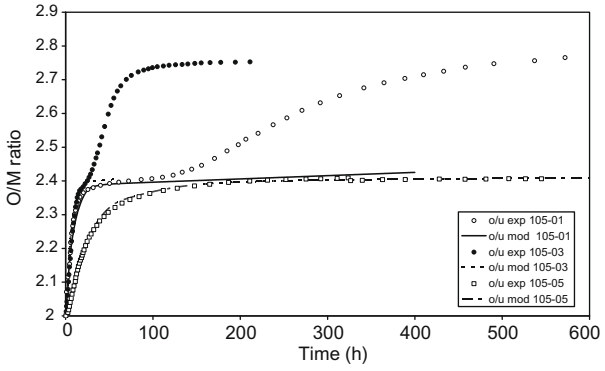

Fig. 9. Comparison between the calculation and the experimental Hanson data [1], different oxidation temperatures.

Table 3
Values of model input parameters.

Literature	T (K)	$D_{U_4O_9}$ ($\mu m^2 s^{-1}$)	$D_{U_4O_{9+y}}$ ($\mu m^2 s^{-1}$)	P	t_0 (h)
Einziger-ATM-104 [10]	468	2.90E-06	3.80E-07	0.386	NC
Einziger-ATM-105 [10]	468	1.60E-06	2.90E-07	0.368	NC
Einziger-ATM-106 [10]	468	9.90E-07	3.50E-07	0.350	NC
Einziger-Turkey Point [10]	468	9.80E-07	1.70E-07	0.344	275
Cadarache-RE2 [6]	473	2.80E-06	2.20E-07	0.448	2000
Cadarache-RE3 [6]	473	2.40E-06	2.75E-07	0.400	1100
Grenoble-LB515 [6]	473	1.00E-05	8.00E-07	0.450	350
Grenoble-LB516 [6]	473	1.00E-05	8.00E-07	0.450	350
Grenoble-LB517 [6]	473	1.00E-05	8.00E-07	0.450	350
Grenoble-LB518 [6]	473	1.00E-05	8.00E-07	0.450	350
Woodley-RUN1 [18]	498	1.30E-05	1.40E-06	0.370	40
Woodley-RUN2 [18]	498	1.50E-05	3.50E-06	0.435	155
Woodley-RUN5 [18]	498	8.00E-06	1.10E-06	0.360	50
Woodley-RUN6 [18]	498	3.00E-06	5.00E-07	0.370	50
Hanson-ATM-105-05 [1]	528	6.00E-05	9.10E-06	0.410	22
Hanson-ATM-105-01 [1]	556	6.50E-05	5.00E-05	0.390	NC
Hanson-ATM-105-03 [1]	581	8.00E-05	7.00E-05	0.400	NC

NC = not calculated because the samples are in powder form. As a consequence the grain boundaries are completely opened.

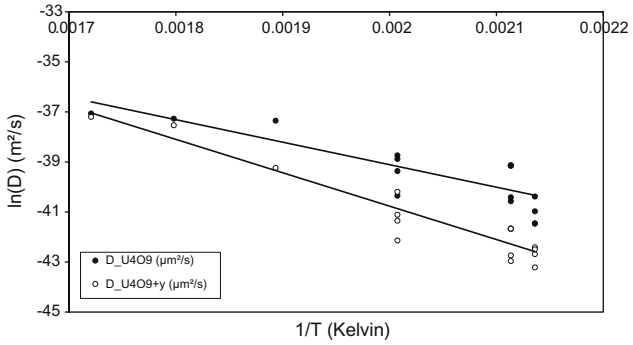

Fig. 10. Arrhenius diagram obtained from adjusting diffusion coefficients obtained in the two phases.

In the modelling, when the stoichiometry (O/M) of U_4O_{9+y} phase reaches a critical value (ε) across a given thickness taken equal to 1 μm the first fracture appears in the grain. Consequently, the numerical calculation gives the instant t_{fract} for which:

$$\frac{O}{M} = 2 + P(1 - \varepsilon) \tag{6}$$

where,

- t_{fract}: the time to have the first fractures;
- ε: critical value of the stoichiometry taken equal to 10^{-3}.
- P: plateau value.

As said beforehand, the rupture criterion chosen shows that the first grain cracks appear in the middle of the oxidation plateau (where a release is observed for RE3, Fig. 5) and thus probably before the spent fuel rod rupture observed during the degradation of a fuel rod slice experiment [7].

On the other hand, calculating a grain cracking time from weight gain curves which have no oxidation plateau (for example if the oxidation test is not long enough, Fig. 8, or if the oxidation temperature is too high and the plateau is nearly absent, Fig. 9)

does not make any sense. As a consequence, the critical time is not calculated in those cases.

The great variability of the "time to reach the centre of the sphere" reflects the disparity of the fragments' size for each sample. The time to fracture (Table 4) are got by choosing ε equal to 0.1%; these times correspond to the moment when the oxidation plateau is well established. The criterion chosen doesn't imply say when the fractures occur but postulates with hypotheses previously explained that they appear for a given advance of the oxidation front. The criterion is chosen to define a degree of advancement of the reaction front (about half plateau) for which no damage on the rod is considered.

4. Discussion

One of the aims of the modelling of the spent fuel oxidation is to link the operational parameters, namely the burn up, the linear power or, the fraction gas released, to the model parameters previously presented ($D_{U_4O_9}(T°)$, $D_{U_4O_{9+y}}(T°)$, R_{eq}, v, t_{fract}). Linking these parameters together enables to propose a so-called operational model, i.e., a simplified model based on mechanisms at stake during oxidation. As shown in the previous paragraph, the data available in the literature are not very numerous and the values of some parameters are lacking. Nevertheless, we will try in this part to put forward various tendencies.

According to the data available in the literature and the experiments carried out by the CEA, it is possible to plot the impact of the operational parameters on the shape of the weight gain curve as illustrated in Fig. 11.

- High linear power
  - More important diffusion tunnel network
  - Small incubation period
  - Increase of the weight gain kinetics
- High release gas fraction
  - Reduction of the quantity of intergranular gas in the sample
  - Increase of the oxidation plateau value
- High burn up
  - Fission products and actinides in great number
  - Lengthening of the plateau duration
  - Slowing down of the oxygen diffusion on the plateau.

Table 4
Values of model output parameters.

Literature	$R_{equivalent}$ (μm)	Time to fracture – t_{fract} (h)
Einziger-ATM-104 [10]	NC	4676
Einziger-ATM-105 [10]	NC	5446
Einziger-ATM-106 [10]	NC	7126
Einziger-Turkey Point [10]	183.3975	6972
Cadarache-RE2 [6]	1333.8	11,928
Cadarache-RE3 [6]	899.8	9251
Grenoble-LB515 [6]	233.415	3276
Grenoble-LB516 [6]	233.415	3276
Grenoble-LB517 [6]	233.415	3276
Grenoble-LB518 [6]	233.415	3276
Woodley-RUN1 [18]	26.676	ND[a]
Woodley-RUN2 [18]	103.3695	ND[a]
Woodley-RUN5 [18]	33.345	ND[a]
Woodley-RUN6 [18]	33.345	ND[a]
Hanson-ATM-105-05 [1]	14.6718	279
Hanson-ATM-105-01 [1]	NC	53
Hanson-ATM-105-03 [1]	NC	ND[b]

NC = not calculated because the samples are in powder form. As a consequence the grain boundaries are completely opened.

[a] ND = not determined because the oxidation plateau is not totally established. As a consequence, it is impossible to determine a fracture time.

[b] ND = not determined because at this temperature, none oxidation plateau exists.

The sample theoretical density or initial porosity that depends on the manufacturing process also has an influence. Indeed, the higher initial porosity is and the higher oxygen access to free surfaces is, and thus a more rapid weight gain is to be expected. In the same way, the grain size may have an impact on oxidation kinetics.

4.1. Operational parameters influence

4.1.1. Influence of the temperature

Fig. 12 shows the effect of temperature on the time necessary to initiate the first crack in the grains, all other parameters kept constants. As expected that time reduces with temperature.

4.1.2. Influence of burn up

Fig. 14 shows the evolution of the time to fracture according to the burn up around 473 K but with a different irradiation history in terms of linear power and FGR. When the burn up increases, t_{frac} increases in the same way (the tendency is even more clear if only the results obtained for burn up higher than 40 GWj t^{-1} are considered, Fig. 13). It is difficult to decide of the influence of burn up with so few data. Nevertheless, it seems that the increase of the burn up entails an increase of that time, which is expected considering the literature data [2]. Indeed, Hanson reports that the plateau's duration may increase by about 3 orders of magnitude according to the concentration of impurities in the fragment, which would also delay the appearance of the first grain cracks. Complementary data are necessary, in particular on high burn up samples, to decide on the influence of burn up on the time to fracture.

Additional measurements of oxidation kinetics with UO_2 doped with various content in rare earths (Gadolinium, Neodymium which is a simulant of Pu...), would enable to validate the increase of the plateau duration and as a consequence the time to appearance of the fractures. Indeed, as reported by Thomas et al. [13], the gadolinia forming the solid solution in the UO_2 matrix stabilizes U_4O_9 and delays U_3O_8 forming. Recent studies also mentioned that the simulated fission products forming the solid solution in UO_2 delayed the appearance of U_3O_8 [24]. Moreover, it would enable to validate oxygen diffusion coefficient values according to the burn up.

The influence of the linear power is difficult to traduce graphically because this data is often missing in the literature. Consequently, this parameter is not introduced into the operational model.

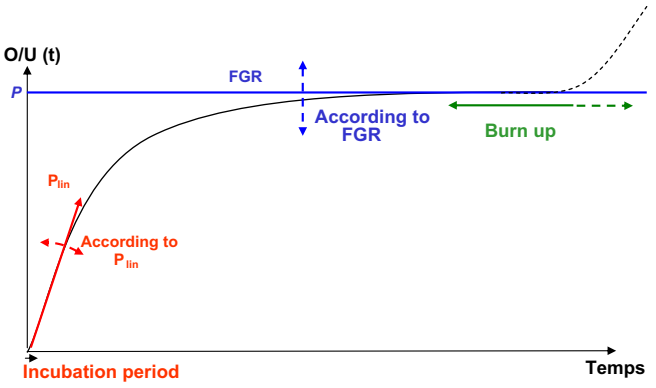

Fig. 11. Schematization of the oxidation kinetics in relation to operational parameters.

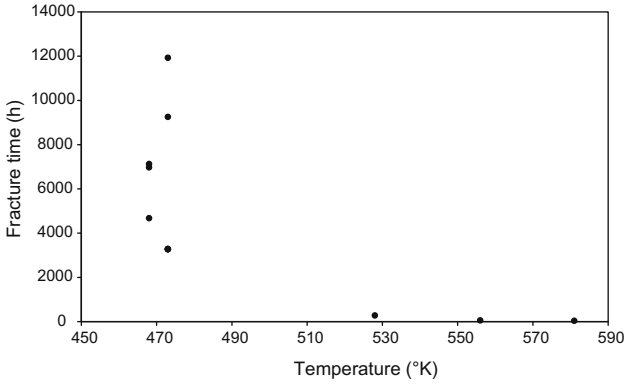

Fig. 12. Time to fracture the grains according to temperature.

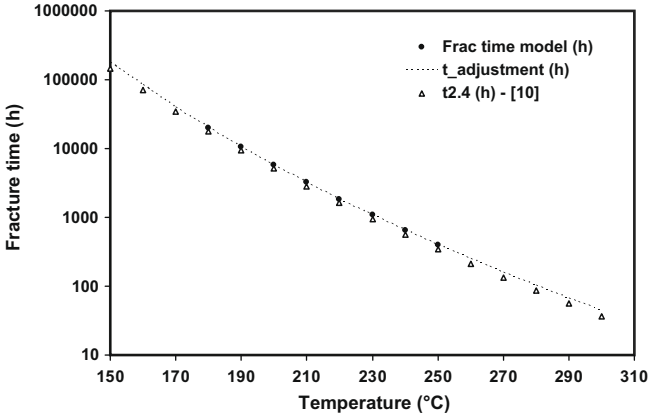

Fig. 14. Comparison between the criterion proposed in this paper and the time ($t_{2.4}$) from Einziger et al. [10].

4.2. Definition of a criterion for the operational model

In Section 4.1 the effects of some irradiation parameters in reactor on the time of appearance of the first cracks in the grain has been shown. In case of accidental contact between the spent fuel and the air, it is necessary to estimate, according to the characteristics of the spent fuels, a majoring time in order to prevent a possible swelling of the matrix being likely to constrain the rod, leading to the initial defect propagation and the release of radionuclides into the atmosphere.

The important point for the operational model is the time from which one begins the fragmentation of UO_2 grains while keeping into account the irradiation history of the fragments. The most favourable case toward this criterion is the following:

- The lowest possible storage temperature bringing about weak oxygen diffusion in the matrix.
- A high burn up, considering the presence of fission products and actinides in great number which hinder oxygen propagation (high plateau duration).
- A low linear power bringing about a relatively sparse tunnel network, which limits oxygen diffusion ways.

The time to fracture the grains, defining the criterion for the operational model, can be described in a predictive way from the oxygen diffusion coefficients in the two phases obtained by adjustments. These diffusion coefficients vary according to the temperature. As has been previously mentioned, it is difficult to give assessed values of a fracturation time according to operational parameters because of a lack of information (initial porosity, grain size...) in the literature's data on the one hand and a lack of experimental data and a big disparity in the samples treated (powders, fragments, mixture of both...) on the other hand. As a consequence, a predictive calculation of the time to fracture can only be realized according to temperature. The values obtained by the model are adjusted by means of a power law to give us the operational model criterion. For a range of oxidation temperatures between 423 and 573 K, the time for the first crack of grains to appear is given by the following analytical formulation, Eq. (7):

$$t_{\text{adjustment}}(h) = 1.938 \times 10^{31}.T^{-11.936} \tag{7}$$

with $R^2 = 1$ and T is the temperature in Celsius.

This criterion is necessarily conservative since it is considered here that the grain boundary oxidation is instantaneous. Considering a weak linear power and a high burn up should delay this time of appearance. It is interesting to compare these values with the literature data in particular those proposed by Einziger et al. [11] which define a waiting time ($t_{2.4}$) to reach the stoichiometry $O/M = 2.4$. This time is a function of temperature and has the following form:

$$t_{2.4}(\text{h}) = 2.6 \times 10^{-9} \exp\left(\frac{111.37\ \text{kJ mol}^{-1}}{RT}\right)$$

The comparison between the criterion proposed in this paper and the time $t_{2.4}$ is given on Fig. 14. The criterion leads to fracture time slightly superior to $t_{2.4}$ which is not surprising since it is in fact chosen to define the reaction front degree of advancement (chosen at about half oxidation plateau) for which no damage of the rod is contemplated.

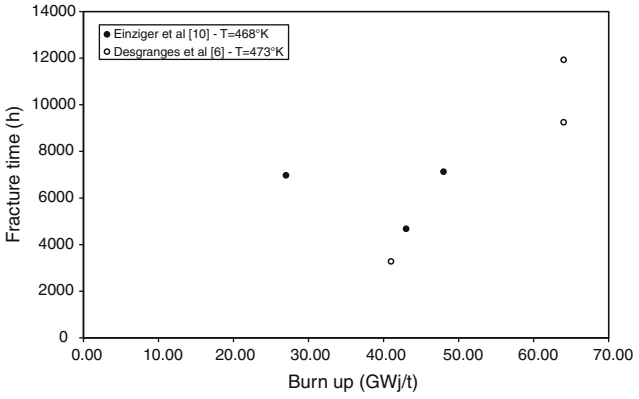

Fig. 13. Time to fracture the grains according to the burn up for a temperature of about 473 K.

5. Conclusion and outlooks

5.1. Sharing pre-existing models

The similarity between the unirradiated fuel and the spent fuel for the series of structural phase changes ($UO_2 \rightarrow U_4O_9 \rightarrow U_4O_{9+y}$) has enabled, thanks to the sensitivity of the grain model at stoichiometric ranges, to model the weight gain of irradiated grains during oxidation. Enhanced by the inclusion of the convolution product between oxygen propagation rate at grain boundaries and the grain model, the model now enables a mechanistic modelling of a spent fuel fragment. It is clear that, to improve and totally validate the model proposed, one should ensure that stoichiome-

tric U_4O_9 exists as an intermediate phase in the spent fuel, which is difficult to check considering the experimental means one must use to study irradiated material. The hypothesis of a constant rate at grain boundaries was made because of lack of experimental data on that subject. It seems obvious that a gas propagation in the diffusion tunnels increases with temperature. In the future, we should use the propagation rate of oxygen at grain boundaries as a parameter varying with temperature, which would enable to physically describe the so-called "closed" grain boundaries oxidation. The parameter of equivalent sphere radius used in the present model would only be used for the description of the so-called "open" grain boundaries. But the counterpart of such an approach is the introduction of another adjustable parameter which is not easy to quantify experimentally. The linear power is also a factor favoring an increase of the rate at grain boundaries by its action of creating some diffusion tunnels. It would be necessary to realize more experiments to reinforce the link between the gas release kinetics and the oxidation kinetics.

5.2. Comparison between the calculation and the experiments

The results show the oxidation model adequately describes the weight gain curves. The numerical adjustment of the physical parameters of oxygen diffusion in the spent fuel is realized. So it has been noticed that the activation energies and the values of the two diffusion coefficients of oxygen in the two phases agreed with the literature data already established on the unirradiated fuel [14]. Indeed, one finds that the spent fuel activation energy (U_4O_9 phase) is more important than for an unirradiated fuel, which may be explained by a slowing down of oxygen progression in the matrix due to fission products. As we have seen, different samples at the same temperature don't have similar diffusion coefficients. A possible way to explain these differences would consists in verifying a dependency relation of the pre-exponential term D_0 (in the Arhenius law) with the burn up, the sample porosity and the y coefficient defining the stoichiometry of U_4O_{9+y} phase. The criterion used for the time of appearance of the first fracture is defined with ε coefficient whose value must be validated by complementary studies either experimentally or by refine models.

5.3. The influence of operating parameters on the cracks criterion

The known effects of the linear power, of the burn up and the temperature could be found on the oxidation curves. Moreover, the relationship between these parameters and the model physical elements make up a first compilation of results. However, better adapted experiments must be imagined to collect more results and hence draw laws on the weight gain according to these parameters.

Finally, a predictive model enabling to obtain a time of appearance of the first fractures according to the temperature is proposed. The impact of the operational parameters such as linear power and burn up on the criterion proposed is difficult to evaluate since too few data are available in the literature and the samples studied are too different. Nevertheless, the criterion obtained predicts times which are quite comparable to those available in the literature [11] with, on top of it, the fact of taking into account, on the one hand, the physical mechanisms at stake during oxidation and, on the other hand, a criterion defining a degree of advancement of the reaction front (corresponding to the middle of the oxidation plateau) for which no damage on the fuel rod is expected. The only operational parameter now considered today in the operational model is the temperature. As a consequence, the model is conservative since the other operational parameters in particular a weak linear power and a high burn up, necessarily slow down the kinetics and lengthen the plateau duration, respectively. To take them into account in a fuller operational model, one should link the equivalent sphere radius to the linear power and the released gas fraction in a more quantitative way. As to the burn up effect, it could be directly integrated in the oxygen diffusion coefficients via the pre-exponential terms in the different structural phases. To that end more oxidation experiments at a fixed temperature for spent fuels at different burn up and identical linear power should be carried out (in order to decorrelate the effects on the oxidation kinetics) and vice versa.

Acknowledgement

The authors are indebted to Electricité de France for their financial support.

References

[1] L. Desgranges, F. Charollais, I. Felines, C. Ferry, J. Radwan, A New Criterion for the Degradation of a Defective Spent Fuel Rod Under Dry Storage Conditions Based on Nuclear Ceramic Cracking, Scientific Basis for Nuclear Waste Management XXXII Meeting, MRS Proceeding, vol. 1124, 2008.
[2] B. Hanson, The Burn Up Dependence of Light Water Reactor Spent Fuel Oxidation, PNNL-11929 Report, 1998.
[3] R.J. McEachern, P. Taylor, J. Nucl. Mater. 254 (1998) 87–121.
[4] G. Rousseau, L. Desgranges, F. Charlot, N. Millot, J.C. Niepce, M. Pijolat, F. Valdivieso, G. Baldinozzi, J.F. Bérar, J. Nucl. Mater. 355 (2006) 10.
[5] A. Poulesquen, Modèle d'oxydation de grains: comparaisons aux données de la littérature, NT DPC/SECR 06-006 indice A, Personal Communication, 2006.
[6] P. Taylor, J. Nucl. Mater. 344 (2005) 206–212.
[7] L. Desgranges, M.P. Ferroud-Plattet, H. Giacalone, I. Aubrun, J.M. Untrau, Bilan des expériences d'oxydation ménagées à 200 °C menées au LECA et au LAMA dans le cadre du programme PRECCI, NT DEC/SA3C/L2EC – 006 – indice 0, Personal Communication, 2007.
[8] L.E. Thomas, R.E. Einziger, R.E. Woodley, J. Nucl. Mater. 166 (1989) 243–251.
[9] I. Zacharie, S. Lansiart, P. Combette, M. Trotabas, M. Coster, M. Groos, J. Nucl. Mater. 255 (1998) 85–91.
[10] K.M. Wasywich, W.H. Hocking, D.W. Shoesmith, P. Taylor, Nucl. Technol. 104 (1992) 309–329.
[11] R.E. Einziger, L.E. Thomas, H.C. Buchanan, R.B. Stout, J. Nucl. Mater. 190 (1992) 53–60.
[12] B. Hanson, Clad Degradation – Dry Unzipping, ANL-EBS-MD-000013 REV 00, 2000.
[13] L.E. Thomas, R.E. Einziger, H.C. Buchanan, J. Nucl. Mater. 201 (1993) 310–319.
[14] A. Poulesquen, L. Desgranges, C. Ferry, J. Nucl. Mater. 362 (2007) 402–410.
[15] A. Poulesquen, L. Desgranges, C. Ferry, Modeling of Spent Fuel Oxidation at Low Temperature, Scientific Basis for Nuclear Waste Management XXX Meeting, MRS Proceeding, vol. 985, 2006.
[16] L. Quemard, L. Desgranges, V. Bouineau, M. Pijolat, G. Baldinozzi, N. Millot, J.C. Niepce, A. Poulesquen, Cracking of the UO2 nuclear spent fuel in oxidizing environment: A kinetic, morphological and structural study, accepted in the Journal of the European Ceramic Society 29 (2009) 2791–2798.
[17] A.H. Booth, A Method of Calculating Fission Gas Diffusion from UO_2 and Its Application to the X-2-F Loop Test, 1957 (AECL CRDC-721).
[18] M. Uchida, J. Nucl. Sci. Technol. 30 (1993) 752–761.
[19] D.J.M. Bevan, I.E. Grey, B.T.M. Willis, J. Solid State Chem. 61 (1986) 1–7.
[20] F. Garrido, R.M. Ibberson, L. Nowick, B.T.M. Willis, J. Nucl. Mater. 322 (2003) 87–89.
[21] P. Menegon, L. Desgranges, Y. Pontillon, A. Poulesquen, J. Nucl. Mater. 378 (2008) 1–8.
[22] R.E. Woodley, R.E. Einziger, H.C. Buchanan, Nucl. Technol. 85 (1989) 74–88.
[23] L. Desgranges, G. Baldinozzi, G. Rousseau, J.-C. Niepce, G. Calvarin, Inorg. Chem. (2009), doi:10.1021/ic9000889.
[24] K.H. Kang, S.H. Na, K.C. Song, S.H. Lee, S.W. Kim, Thermochim. Acta 455 (2007) 129–133.